

SELF v1.0: A minimal physical model for predicting time of freeze-up in lakes

– Supplementary Material –

Marco Toffolon¹, Luca Cortese^{1,2}, and Damien Bouffard²

¹Department of Civil, Environmental and Mechanical Engineering, University of Trento, Italy

²Eawag, Swiss Federal Institute of Aquatic Sciences, Department Surface Waters Research & Management, Kastanienbaum, Switzerland

Correspondence: Marco Toffolon (marco.toffolon@unitn.it), Damien Bouffard (Damien.Bouffard@eawag.ch)

Outline. This document contains

- Section S.1: discussion on the energy balance;
- Section S.2: discussion on the physical interpretation of the calibration parameter of SELF;
- Section S.3: simplified version of SELF that allows for an analytical solution;
- 5 – Section S.4: summary of the performances of Simstrat vs. the available observations;
- Section S.5.1: interannual variability of the day with LSWT = 4°C and ice-on date;
- Section S.5.2: statistical distributions of the duration of the pre-freezing period;
- Section S.5.3: results obtained with SELF for the lakes not included in the main text;
- Section S.5.4: correlation of the pre-freezing duration with negative degree days.

10 S.1 Energy considerations

S.1.1 Thermal and mechanical energy

We consider a water column with variable density $\rho(z, t)$ [kg m^{-3}] and temperature $T(z, t)$ [$^{\circ}\text{C}$], linked via a non-linear equation of state (equation 2 in the main text), in a gravitational field with acceleration g [m s^{-2}], where z [m] is the vertical coordinate pointing downwards. The bulk energy balance of the system should include both mechanical (potential E_{pot} and kinetic E_{kin}) and internal (thermal) energy E_{int} per unit area [J m^{-2}], together with the energy fluxes [W m^{-2}] given by the net heat flux H_{net} and the wind power P_{wl} effectively transferred to the lake. The most general version of the energy equation for the water volume considered as a thermodynamic system reads:

$$\frac{d}{dt}(E_{int} + E_{pot} + E_{kin}) = H_{net} + P_{wl}, \quad (\text{S.1})$$

where $E_{int} = E_{int,0} + \int \rho(T)c_p T dz$, with $c_p \simeq 4.2 \text{ kJ } ^{\circ}\text{C}^{-1} \text{ kg}^{-1}$ the heat capacity of water at constant pressure and $E_{int,0}$ a suitably defined constant, and $E_{pot} = E_{pot,0} - \int \rho(T)gz dz$ can be defined with respect to an arbitrary reference state (z pointing downwards). Note that $P_{wl} < P_w$, where $P_w = \rho_a C_D W^3$ is the wind power estimated in the atmosphere at a conventional height above the lake's free surface (see equation 4 in the main text and the discussion in section S.2 below).

Different orders of magnitude are involved in the balance expressed by equation (S.1): just to give an example, if the temperature changes by 0.5°C (implying a density changes $\sim 10^{-2} \text{ kg m}^{-3}$) uniformly over a depth of 5 m in 1 day, then $dE_{int}/dt \sim 10^2 \text{ W m}^{-2}$; $dE_{pot}/dt \sim 10^{-5} \text{ W m}^{-2}$. It is more difficult to give a meaningful estimation of dE_{kin}/dt , which might be on the same order of dE_{pot}/dt . In this simplified description of the energy balance, we assume that the change of kinetic energy from day to day is minor, and we do not consider a momentum balance. Hence, we simplify equation (S.1) by neglecting the term dE_{kin}/dt , and evaluate each term of the right hand side separately. Interpreting the assumption in terms of the terminology used, e.g., by Winters et al. (1995), we are focusing on the balance of the background potential energy neglecting the adiabatic changes in available potential energy due to the kinetic energy of the flow.

The mechanical energy budget is classically partitioned between a heating/cooling term and a wind-induced mixing term (Simpson et al., 1978), which we set here in integral terms as

$$\Delta E_{pot} \simeq \frac{\partial E_{pot}}{\partial E_{int}} \Delta E_{int} + \int \eta P_w dt, \quad (\text{S.2})$$

where $\partial E_{pot}/\partial E_{int}$ formally expresses how the change in the thermal energy modifies the potential energy, via the equation of state, and η is the model's coefficient that requires a calibration. In equation (S.2), the rate of change of the potential energy due to the change of temperature dominates the stratification process, while the wind power is responsible for the destratification. However, not all the wind power is made available to modify the potential energy, but only a tiny fraction ηP_w , where the efficiency $\eta \ll 1$. The remaining part, $P_{wl} - \eta P_w$, causes mixing and, eventually, is dissipated into heat by means of molecular viscosity at the small (Kolmogorov) scales at which the mechanical energy is transferred by turbulence. Thus, it should enter into the thermal energy budget,

$$\Delta E_{int} \simeq \int H_{net} dt + \int (P_{wl} - \eta P_w) dt, \quad (\text{S.3})$$

but its magnitude ($\sim 10^{-2} - 10^{-1} \text{ W m}^{-2}$) is some orders of magnitude smaller than H_{net} ($\sim 10^2 \text{ W m}^{-2}$), which primarily governs the temperature dynamics. Practically, the last term in equation (S.3) is neglected as in the widely used equation:

$$\Delta E_{int} \simeq \int H_{net} dt. \quad (\text{S.4})$$

45 This separation between internal and mechanical energy is common to the majority of the models, where the heat balance is independent of the momentum equation (e.g., as in Simstrat; see Goudsmit et al. 2002). In addition, we introduce another assumption in the minimal model, which is crucial to highlight the role of the different processes: we further simplify the equation describing the temporal change in E_{pot} (equation S.2) by attributing the two terms in the right-hand side of the equation to two decorrelated phases. The phase A represents the wind-induced mixing of the surface layer, previously stratified
50 as a result of the change of potential energy due to the heat flux in phase B (see Figure 1 in the main text). Therefore, equation (S.2) is simplified for phase A as

$$\Delta E_{pot} \simeq \int \eta P_w dt, \quad (\text{S.5})$$

while in phase B we directly assign the temperature profile, which modifies the water density and, eventually, the mass distribution and the potential energy. The separation of the two processes over a suitable time scale is the core of the minimal
55 model.

S.1.2 Alternative formulation of the heat budget

A particular case of equation (S.1) can be formulated in a simplified way that might be more familiar to some readers. Assuming that the variables involved in the heat budget are uniformly distributed along the water column (having depth h), it is possible to express the variation of internal energy as $dE_{int}/dt \simeq \rho c_p h dT/dt$ and the potential energy can be estimated as $E_{pot} \simeq$
60 $\rho g h^2/2$. Imposing mass conservation (such that $M = \rho h$ is constant, per unit surface), $E_{pot} \simeq g M^2/(2\rho)$ and its variation is $dE_{pot}/dt \simeq -gh^2 d\rho/dt/2$. Thus, neglecting also the kinetic energy, the simplified heat budget reads

$$\left(c_p + \frac{gh\alpha}{2} \right) \rho h \frac{dT}{dt} = H_{net} + P_{wl}, \quad (\text{S.6})$$

where $\alpha = -\rho^{-1} d\rho/dT$ is the thermal expansion coefficient. For $\alpha \sim 10^{-6} \text{ K}^{-1}$, $g \sim 10 \text{ m s}^{-2}$ and $h \sim 10 \text{ m}$, the second term within brackets is $\sim 10^{-4} \text{ J kg}^{-1} \text{ K}^{-1}$, which is much smaller than $c_p \sim 10^3 \text{ J kg}^{-1} \text{ K}^{-1}$. This confirms that different order of
65 magnitudes between the rates of change of internal and potential energy.

Note that $\alpha < 0$ for $T < T_{md}$ (the conditions we are investigating), so a cooling ($dT/dt < 0$) reduces the internal energy but slightly increases the potential energy because the density decreases and the volume expands. However, equation (S.6) does not consider the effect of stratification (ρ varies along the vertical) whereby the different distribution of the mass affects the potential energy.

70 S.1.3 Energy required to mix the surface layer in phase A

As explained in the main text, the wind can provide the energy necessary to destratify the water column. In this section, we show how the potential energy changes passing from a linear stratification to well-mixed conditions. To this end, we temporarily

adopt a different notation, with a coordinate y pointing upwards with origin at the base of the layer that is actually being mixed.

With this notation, the potential energy is defined as

$$75 \quad E_{pot} = \int_0^h \rho g y dy, \quad (S.7)$$

where h is the distance from the base of the layer to the free surface.

Let us first assume the the water volume is conserved (hence h does not vary in the destratification process) and consider a linear variability of the density

$$\rho(y) = \rho_d (1 - \sigma y), \quad (S.8)$$

80 where ρ_d is the density at the bottom of the layer and $\sigma > 0$ to have a stable stratification. The initial state is characterized by a potential energy $E_{pot,1} = \rho_d g h^2 (1/2 + \sigma h/4)$. In the final state, after the complete destratification, the density becomes uniformly equal to $\rho = \rho_d (1 - \sigma h/2)$, so the energy is $E_{pot,2} = \rho_d g h^2 (1/2 + \sigma h/3)$. Thus, the difference of potential energy is

$$\Delta E_{pot} = E_{pot,2} - E_{pot,1} = \frac{\rho_d g \sigma h^3}{12} > 0, \quad (S.9)$$

85 which demonstrates the inequality reported in the main text, stating that there is a need of external energy to destratify the water column.

In order to develop a more rigorous analysis, we can also relax the assumption of volume conservation (typical of practically all numerical models), which would correspond to keep h constant, and adopt to the physically sounder requirement of mass conservation, where the mass per unit area is $M = \int_0^h \rho dy$. Furthermore, instead of the linear variation of density described by

90 equation (S.8), we consider a linear temperature profile

$$T(y) = T_d - \delta y, \quad (S.10)$$

with T_d the temperature at the bottom of the layer and δ the temperature gradient ($\delta > 0$ in the cooling phase). We assume the parabolic equation of state (equation 2 in the main text), so that $\rho_d = \rho_{max} + a_0 + a_1 T_d + a_2 T_d^2$, with ρ_{max} the water density at $\simeq 4^\circ\text{C}$. As a result of the mixing, the final uniform temperature would be $T = T_d - \delta h/2$. We can study the energy change

95 by following the same procedure as above, but distinguishing between the initial (h_1) and final (h_2) layer thickness. The mass conservation principle leads to a complicated algebraic condition, which however predicts that $h_2 < h_1$, although the difference is typically irrelevant for the problem we deal with. Similarly, it is not worth reporting the complete algebraic equation for the difference of potential energy, but it suffices to say that, also in this case, $\Delta E_{pot} = E_{pot,2} - E_{pot,1} > 0$ and the difference is close to the value predicted by equation (S.9).

100 S.1.4 Development of the stratification in phase B and variation of potential energy

Phase B describes the process whereby the stratification is established. The assumption of a linear stratification is only a rough description of what is likely to happen in reality. The idealized model behind the process refers to a layer of water

characterized by a relatively intense turbulent diffusion (the well-mixed layer at the surface), lying on top of another layer where the temperature is approximately constant. We assume that the heat exchanged at the air-water interface produces a diffusive flux in the surface layer.

Under steady conditions, the resulting temperature profile would be linear, as described in equation (S.10). Based on simple theoretical arguments for diffusive processes, the time scale to reach a steady state is $\mathcal{T}_D \sim h^2/K$, with K a reference value of the vertical eddy diffusivity. Assuming $h \sim 10$ m and $K \sim 10^{-3} \text{ m}^2 \text{ s}^{-1}$, the time scale $\mathcal{T}_D \sim 1$ day, which corresponds to the time step of the model. For a shallower surface layer or more intense turbulence, shorter times would be required.

The way the potential energy changes in phase B is not completely obvious. We start from a uniform temperature profile ($T = T_d$ and $\rho = \rho_d$ in the layer of thickness h_1) and we end up with a linear stratification. Let us first consider the case where the volume is conserved ($h_2 = h_1$, note that this is the usual assumption in numerical models) and the final ρ varies linearly as in equation (S.8). The difference $\Delta E_{pot} = -\rho_d g \sigma h^3/3$, which implies that the potential energy should decrease because the water at the top of the layer becomes lighter. However, this result is not correct because the expansion of the water is neglected.

If one imposes mass conservation, instead, the result is opposite: potential energy increases. In fact, the thickness increases ($h_2 > h_1$, although the difference is infinitesimal), as can be seen using (S.8) to derive that $h_1 = h_2(1 - \sigma h_2/2)$. Then, the difference $\Delta E_{pot} = \rho_d g \sigma h_2^3(1/6 - \sigma h_2/8)$ is typically a positive number because $\sigma \sim 10^{-5} \text{ m}^{-1}$ in typical conditions. The potential energy grows if the layer stably stratifies because the centre of mass uplifts slightly. Similar results can be obtained using (S.10), but the solutions are algebraically more complicated.

120 S.2 Physical interpretation of the calibration parameter

In this section, we analyze the process of energy transfer from the wind to the lake, and in particular how to estimate the energy of the surface currents in a lake. Neglecting the effect of Earth rotation, assuming a constant value for the reference vertical eddy viscosity ν_z [m s^{-2}], and referring to steady-state conditions, the velocity profile can be obtained analytically (Heaps, 1984). Different approximations can be invoked. Here we consider the case of a no-slip condition at the bottom, which can be a simplified model for a surface layer on the top of a strongly stratified layer (Toffolon and Rizzi, 2009). Then, the velocity at the free surface is

$$U = \frac{1}{4} \frac{\tau h_f}{\rho_0 \nu_z}, \quad (\text{S.11})$$

where h_f [m] is the depth over which the surface flow develops.

Selecting an appropriate constant value for ν_z is the most complex task. As a first approximation, we assume a parabolic profile $\nu_z = \kappa u_* z(1 - z/h_t)$ as a function of the distance z from the free surface, over the depth h_t affected by turbulence (which scales with h_f), and average it to obtain

$$\nu_z = \frac{\kappa}{6} u_* h_t, \quad (\text{S.12})$$

where $\kappa \simeq 0.4$ is the von Kármán constant and $u_* = \sqrt{\tau/\rho_0}$ [m s^{-1}] is the friction velocity.

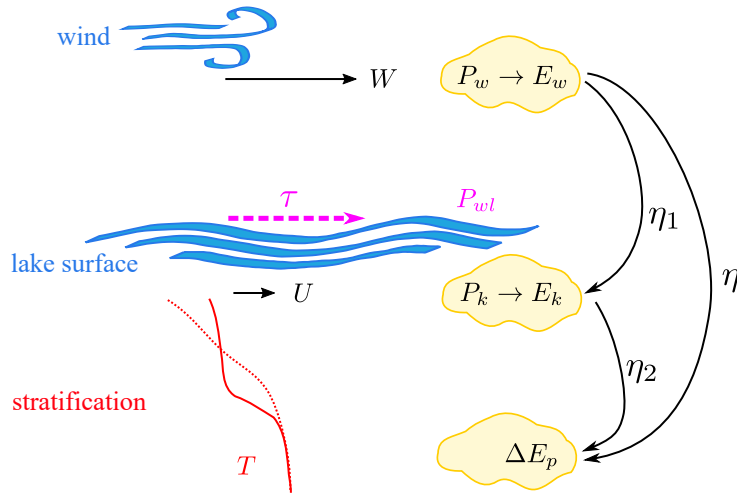


Figure S.1. Conceptual scheme of the energy transfer from the wind energy, E_w , to the energy at the lake surface, E_k , to the change of potential energy in the stratified water column, ΔE_p .

Combining equations (S.11) and (S.12), it follows that

$$135 \quad U = \frac{3}{2\kappa} \frac{h_f}{h_t} u_* , \quad (\text{S.13})$$

so that the rate of working $P_k = \tau U$ [W m^{-2}] can be estimated as

$$P_k = \frac{3}{2\kappa} \frac{h_f}{h_t} \sqrt{\frac{\rho_a}{\rho_0}} C_D \rho_a C_D W^3 = \gamma W^3 . \quad (\text{S.14})$$

Note that $P_k < P_{wl}$ because part of the wind power transferred to the lake (P_{wl}) is dissipated at the surface (by breaking waves, Stokes dissipation, etc.) and does not contribute to the development of surface currents. Assuming that $h_t \simeq h_f$, it is possible
 140 to obtain the order of magnitude of $\gamma = 3/2\kappa \sqrt{\frac{\rho_a^3}{\rho_0}} C_D^{3/2} \simeq 0.8 \times 10^{-5} \text{ kg m}^{-3}$.

Thus, the mechanical energy E_k [$\text{J m}^{-2} \text{ day}^{-1}$] transmitted from the wind to the water can be obtained as

$$E_k = \langle \gamma W^3 \rangle \Delta t , \quad (\text{S.15})$$

where angle brackets denote the temporal average over the time window Δt . However, not the whole input of energy P_w [W m^{-2}] from the wind is transmitted to the water flow. In fact, the ratio η_1 between the rates of working is

$$145 \quad \eta_1 = \frac{P_k}{P_w} = \frac{3}{2\kappa} \frac{h_f}{h_t} \sqrt{\frac{\rho_a}{\rho_0}} C_D . \quad (\text{S.16})$$

A reference value of $\eta_1 \simeq 0.0048$ can be obtained (assuming again $h_t \simeq h_f$) and falls within the range recently proposed for mixed (0.0013) and stratified (0.0064) lakes by Woolway and Simpson (2017). The same coefficient holds for the ratio

between the surface current velocity and the wind speed, so that $U = \eta_1 W$, where η_1 also depends on W through C_D . This estimate of η_1 is an order of magnitude smaller than that proposed for the sea by Kullenberg (1976). Similarly, the range of variation of $\gamma \sim (1 - 5) \times 10^{-5} \text{ kg m}^{-3}$ reported by Imboden and Wüest (1995) is larger than the one derived from the approximate scaling in the present analysis, which however is consistent with the recent estimates by Woolway and Simpson (2017). Nonetheless, any possible shortcoming in the estimation of γ or η_1 has to be connected with the uncertainty in the estimation of $\eta_2 = \Delta E_p / E_k$ (see Figure S.1 for a conceptual summary). Thus, it is more suitable to condense both effects in a single calibration parameter, the global efficiency η , which multiplies the wind energy E_w to obtain the energy ΔE_p effectively available for the destratification of the water column (see equation 5 in the main text).

S.3 Approximate analytical model

S.3.1 Derivation of the linearized model

In this section, we derive a simplified analytical model to obtain a solution in closed form for the case of constant forcing (fixed values of cooling E_c and wind-induced mixing ΔE_p). The whole analysis is based on a daily time interval Δt ; hence, the energies are expressed per unit area and per day [$\text{J m}^{-2} \text{ day}^{-1}$].

As in equation (S.10) and for the SELF model, we assume a linear temperature profile in a layer of height h :

$$T(z) = T_s + \delta z, \quad (\text{S.17})$$

where T_s is the surface temperature and $\delta = \Delta T / h$ [$^\circ\text{C m}^{-1}$] the vertical gradient, with $\Delta T > 0$ the decrease of surface temperature for the case of cooling (hence, $\delta > 0$). Accordingly, the energy that has to be extracted from the surface layer to produce the linear temperature profile (S.17) is

$$E_c = \frac{\rho_0 c_p h \Delta T}{2}. \quad (\text{S.18})$$

In order to derive an explicit analytical solution, we need to introduce a few strong assumptions. First, we assume a linear variation of water density with temperature:

$$\rho(T) = b_0 + b_1 T \quad (\text{S.19})$$

where the coefficients are different from those of the parabolic equation (2) in the main text. Although the linear variation is not representative of the actual equation of state, which should be approximated at least by a parabolic function, it is needed to obtain an analytical result because it allows for removing the effect of temperature on the potential energy change.

The potential energy of the water column E_p is given by equation (3) in the main text. In the case of linear stratification in a layer of thickness h , it reads

$$E_{p,s} = -\frac{gh^2}{2} \left(b_0 + b_1 T_s + \frac{2}{3} b_1 \delta h \right) \quad (\text{S.20})$$

and, after mixing to the constant average temperature $T_s + \delta h/2$, becomes

$$E_{p,m} = -\frac{gh^2}{2} \left(b_0 + b_1 T_s + \frac{1}{2} b_1 \delta h \right). \quad (\text{S.21})$$

Assuming that h does not change in phase A (for a discussion on the implications see section S.1.3), the energy difference from stratified to mixed conditions is

$$180 \quad \Delta E_p = E_{p,m} - E_{p,s} = \frac{b_1 g \delta h^3}{12}, \quad (\text{S.22})$$

which is independent of the temperature thanks to the linearity of the fit (S.19).

In order to describe the evolution of the surface temperature, we consider a sequence of daily steps, as schematically represented in Figure 1 in the main text and Figure S.2 here. Let us assume that, at time t_i , the stratification begins with a thermal gradient (Figure S.2a)

$$185 \quad \delta_i = \frac{\Delta T_i}{h_i} = \frac{2E_c}{\rho_0 c_p h_i^2}, \quad (\text{S.23})$$

as obtained from equation (S.18) for phase B, and continues with the homogenization due to the wind action (phase A, Figure S.2b), producing a new mixed layer with a different height according to equation (S.22):

$$h_{i+1} = \left(\frac{12\Delta E_p}{b_1 \delta_i g} \right)^{1/3}. \quad (\text{S.24})$$

Then, the stratification develops again (Figure S.2c) and the process iterates. We recall that E_c and ΔE_p do not change with
190 time in this simplified description.

Equations (S.23) and (S.24) can be cast in dimensionless form (indicated with a superscript *) introducing $h_i^* = h_i/h_0$ (and analogously for h_{i+1}):

$$\delta_i = \frac{2E_c}{\rho_0 c_p h_0^2} h_i^{*-2}, \quad h_{i+1}^* = \left(\frac{12\Delta E_p}{b_1 g h_0^3} \right)^{1/3} \delta_i^{-1/3}. \quad (\text{S.25})$$

Substituting δ_i from the former into the latter, a relation is obtained for the evolution of the well-mixed layer thickness:

$$195 \quad h_{i+1}^* = \beta h_i^{*m}, \quad (\text{S.26})$$

where $m = 2/3$ and a dimensionless coefficient appears:

$$\beta = \left(\frac{6\rho_0 C_p \Delta E_p}{b_1 g E_c h_0} \right)^{1/3}. \quad (\text{S.27})$$

The relationship (S.26) is used to predict the evolution of the thickness of the mixed layer in one step. The dimensionless coefficient β regulates the velocity at which the mixed layer becomes thinner. Starting from $h_{i=0} = h_0$, hence $h_0^* = 1$, we can
200 compute the layer height at the time step $i + 1 = n$ as

$$h_n^* = \beta^{\theta_n}, \quad (\text{S.28})$$

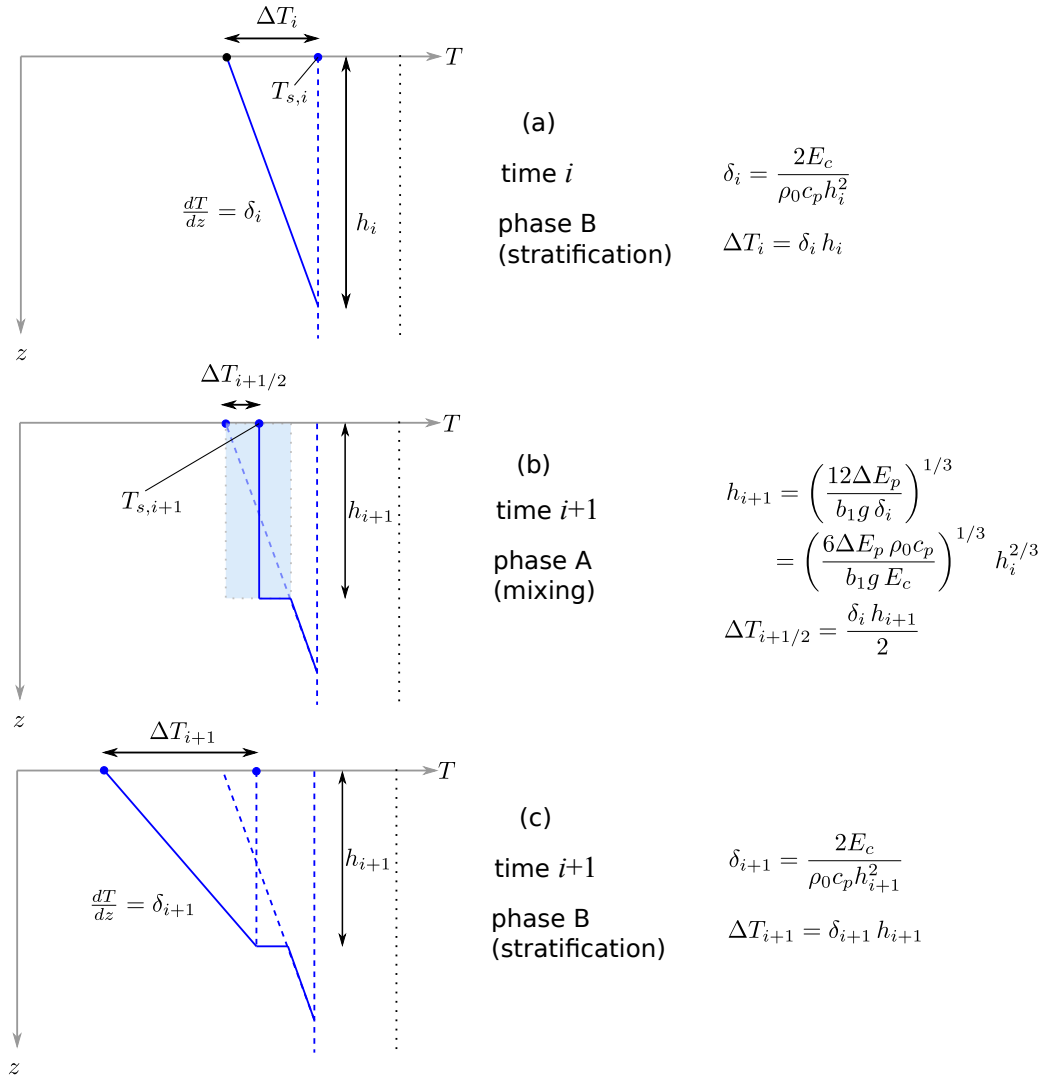


Figure S.2. Sequence of phases showing how the temperature profile evolves in time: (a) starting from a well-mixed condition at time i , a stratification is formed (phase B); (b) wind provides the energy to mix the surface layer, whose thickness changes with respect to that at the previous time (phase A at time $i + 1$); (c) the surface layer stratifies again (phase B at time $i + 1$).

with exponent

$$\theta_n = \sum_{i=0}^{n-1} m^i = \frac{1-m^n}{1-m} \quad (\text{S.29})$$

205 passing from the value 0 for $n = 0$ (initial condition) to 3 asymptotically for $n \gg 1$. Hence, the condition $\beta < 1$ produces an acceleration of the thinning of the mixed layer at each time step. The problem is how to determine the number n of steps (days) to reach the formation of ice, which depends on the behaviour of the surface temperature.

The surface temperature changes from day i to day $i + 1$. Starting from a well mixed condition, stratification forms (Figure S.2a) and the new surface layer is mixed (Figure S.2b). Hence, the change of surface temperature in a day is:

$$T_{s,i+1} - T_{s,i} = -\Delta T_i + \frac{\delta_i h_{i+1}}{2} = -\frac{2E_c}{\rho_0 c_p h_i} + \frac{2E_c}{\rho_0 c_p h_i^2} \frac{h_{i+1}}{2} = -\frac{\Delta T_0}{h_i^*} \left(1 - \frac{h_{i+1}^*}{2h_i^*} \right), \quad (\text{S.30})$$

210 where $\Delta T_0 = 2E_c/(\rho_0 c_p h_0)$ is consistent with the definition (S.18). Then, it is possible to compute the evolution of the surface temperature by using equations (S.26) and (S.28):

$$T_{s,i+1} - T_{s,i} = -\frac{\Delta T_0}{h_i^*} \left(1 - \frac{\beta h_i^{*m-1}}{2} \right) = -\frac{\Delta T_0}{\beta^{\theta_i}} \left(1 - \frac{\beta \beta^{\theta_i(m-1)}}{2} \right) = -\Delta T_0 \Psi_i, \quad (\text{S.31})$$

where

$$\Psi_i = \beta^{-\theta_i} \left(1 - \frac{1}{2} \beta^{1-\theta_i(1-m)} \right) = \beta^{-\theta_i} \left(1 - \frac{1}{2} \beta^{(m^i)} \right). \quad (\text{S.32})$$

215 S.3.2 Approximate estimate of the duration of the pre-freezing period

If the initial value of the surface temperature is approximately 4°C, ice forms when the sequence of n_d days brings it to 0°C, hence for a total difference $\Delta T_{ice} = 4^\circ\text{C}$, so that $\sum_{i=0}^{n_d} \Delta T_0 \Psi_i = \Delta T_{ice}$ from equation (S.31). Introducing the parameter $\Gamma = \Delta T_{ice}/\Delta T_0$, which is dimensionally expressed as number of days, the problem can be cast in dimensionless form as

$$\sum_{i=0}^{n_d} \Psi_i = \Gamma, \quad (\text{S.33})$$

220 which shows that two dimensionless parameters (β and Γ) govern the number of days n_d required to form the ice.

We can look at the properties of the function Ψ_i defined in (S.32). Figure S.3 shows that the function has a horizontal asymptote Ψ_∞ for large i , and initial value Ψ_0 and slope $d\Psi/di = y_s$ for $i = 0$:

$$\Psi_\infty = \frac{1}{2} \beta^{-1/(1-m)}, \quad \Psi_0 = 1 - \frac{\beta}{2}, \quad \Psi_s = \frac{2 + m\beta - 2\beta}{2(1-m)} \log m \log \beta. \quad (\text{S.34})$$

Note that, for the actual value $m = 2/3$, the value of $\Psi_\infty = (2\beta^3)^{-1}$.

225 Assuming the asymptotic value as a constant, a rough approximation for the whole process if it is not long enough, we obtain an estimate of the number of days of the pre-freezing period

$$\Gamma \simeq \sum_{i=0}^{n_d} \Psi_\infty = (n_d + 1) \Psi_\infty \simeq n_d \Psi_\infty = \frac{n_d}{2\beta^3}, \quad (\text{S.35})$$

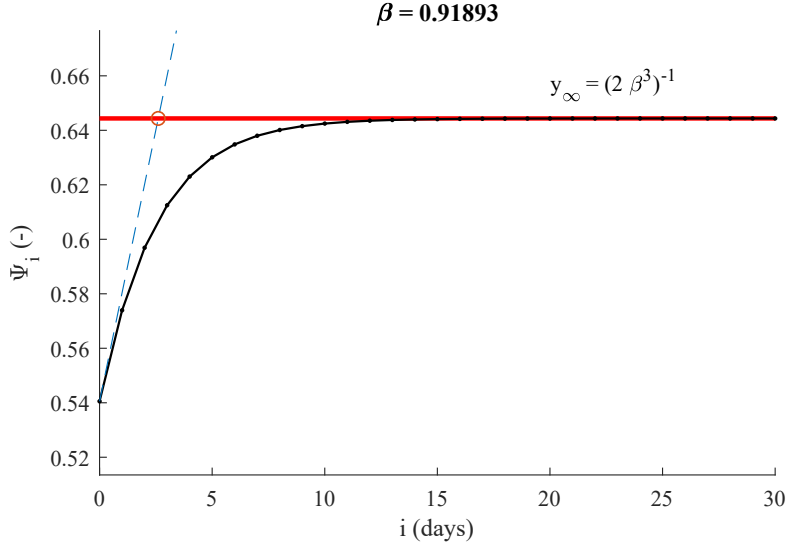


Figure S.3. An example of the function Ψ_i (equation S.32) and asymptotic value Ψ_∞ used to derive the simplified analytical solution for constant forcing, for a given value of $\beta \simeq 0.92$.

where we also have assumed that n_d is sufficiently large. Hence,

$$n_d \simeq 2\Gamma \beta^3 = \frac{6\rho_0^2 c_p^2 \Delta T_{ice} \Delta E_p}{b_{1g} E_c^2} = r \frac{\Delta E_p}{E_c^2}, \quad (\text{S.36})$$

230 where $r = 6\rho_0^2 c_p^2 \Delta T_{ice} (b_{1g})^{-1} \simeq 1.3 \times 10^{15} \text{ kg s}^{-2}$ is approximately a constant. We stress the fact that equation (S.36) cannot give a precise value because of the strong assumptions introduced in the derivation, but at least the order of magnitude of the estimate. Thus, we can recast it as

$$n_d = \mu r \frac{\Delta E_p}{E_c^2}, \quad (\text{S.37})$$

where we have introduced a correction factor $\mu \sim O(1)$ to remind that it is not exact.

235 Equation (S.37) yields n_d given the effective mixing energy per day ΔE_p and cooling per day E_c . The cumulative values [J m⁻²] over the pre-freezing period of n_d days are simply $\Delta E_p^{(n_d)} = \Delta E_p n_d$ and $E_c^{(n_d)} = E_c n_d$. Hence, we can manipulate equation (S.37) to highlight the cumulative energies:

$$E_c^2 n_d^2 = \mu r \Delta E_p n_d, \quad (\text{S.38})$$

which shows that it can be cast as a power law between them, say

$$240 \Delta E_p^{(n_d)} = k \left(E_c^{(n_d)} \right)^2 \quad (\text{S.39})$$

where $k = (\mu r)^{-1}$. Equation (S.39) corresponds to equation (10) in the main text.

S.3.3 Connection with formulations based on negative degree days

If we accept that equation (S.37) provides a first approximation of the conditions for freezing, we can try to connect it to the widely used approach based on negative degree days. In this analysis, we rely again on the assumption of constant daily
 245 energy fluxes E_c and $\Delta E_p = \eta W^3 \Delta t$. Furthermore, we introduce a simplified closure based on the difference between air temperature T_a and LSWT, $E_c \simeq \rho_0 c_p \phi (T_s - T_a) \Delta t$, with ϕ [m s^{-1}] a bulk heat exchange coefficient. Recalling equation (9) of the main text for the definition of negative degree days, and assuming a mean value of air temperature, we can estimate that $D \simeq -n_d T_a$. Finally, neglecting the effect of surface water temperature, we obtain that $E_c \simeq \phi \rho_0 c_p \Delta t D / n_d$. Hence, equation (S.37) becomes

$$250 \quad n_d = \mu \frac{6\Delta T_{ice}}{b_{1g}} \frac{\eta W^3}{\phi^2 D^2 \Delta t} n_d^2 \quad (\text{S.40})$$

and it follows that

$$D = \sqrt{\frac{6\Delta T_{ice} \mu}{b_{1g} \phi^2 \Delta t}} \eta W^{3/2} n_d \quad (\text{S.41})$$

which suggests that any model based only on the computation of negative degree days, D , is incomplete because it misses the effect of wind speed, W , whose dependence is even more than linear.

Table S.1. Root mean square error (RMSE) and R^2 scores of the results of Simstrat against the available observations of water temperature.

Lake	Years	R^2	RMSE [°C]
Sils	2016-2020	0.83	0.26
Silvaplana	2016-2020	0.90	0.21
St. Moritz	2016-2020	0.72	0.29
Joux	2013-2019	0.89	0.17
Sihl	2015-2016	0.93	0.19

255 S.4 Performances of Simstrat

The results of the 1D model Simstrat were compared with the available data of water temperature in the five investigated lakes. The results are reported in Table S.1.

Moreover, in Figure S.4 we report the whole series of temperature profiles obtained for Lake Sils in winter 2016/17, completing the plots shown in Figure 4 of the main text.

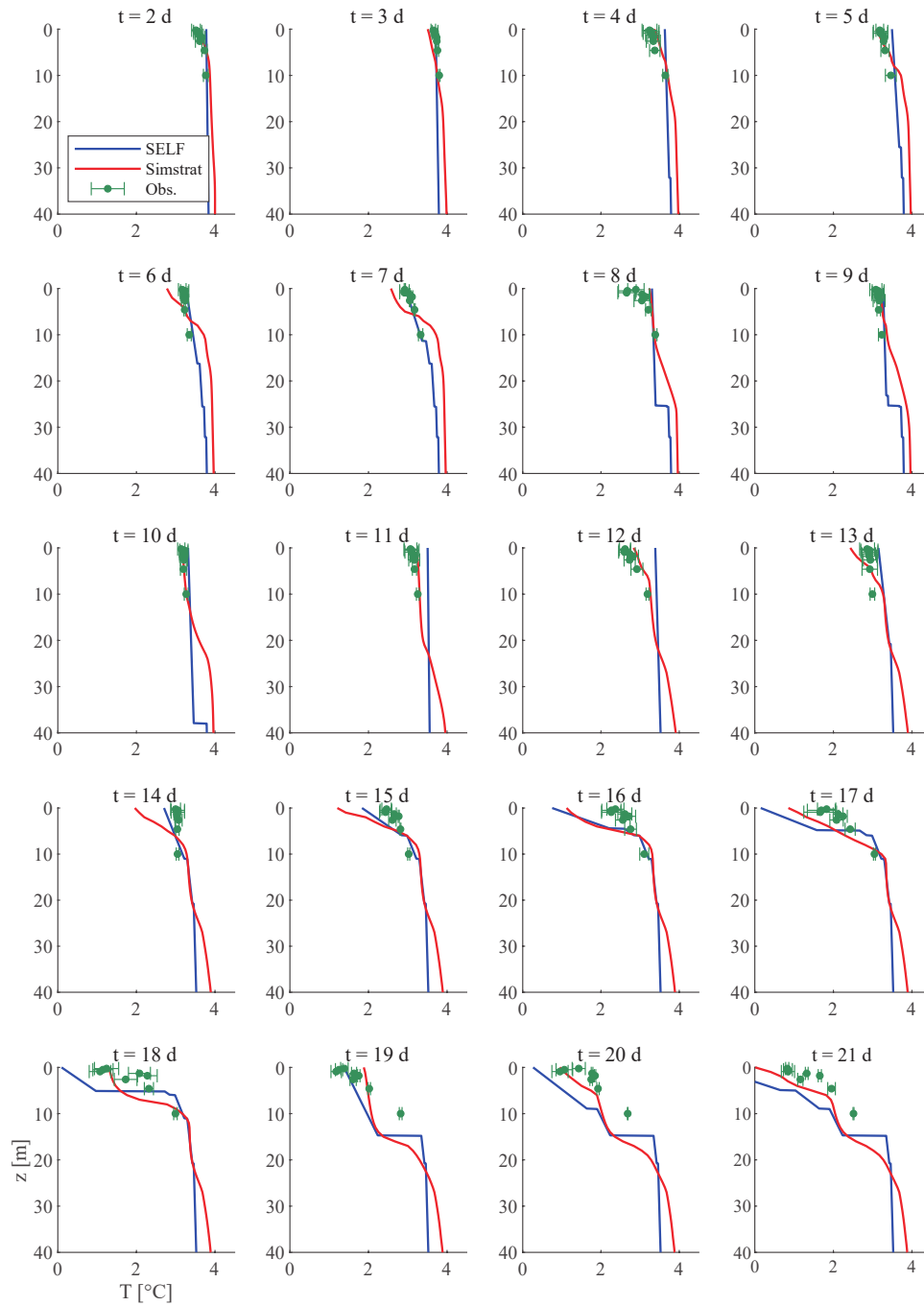


Figure S.4. Evolution of the temperature profile in the pre-freezing period for Lake Sils between 18 December 2016 and 08 January 2017. The plots represent the daily profiles obtained with SELF compared with the profiles at midnight computed by Simstrat. The dotted lines represent the SELF model's temperature profile on the previous day. The symbols represent the available observations, with the error band equal to one standard deviation of the temperature during the day.

S.5.1 Interannual variability

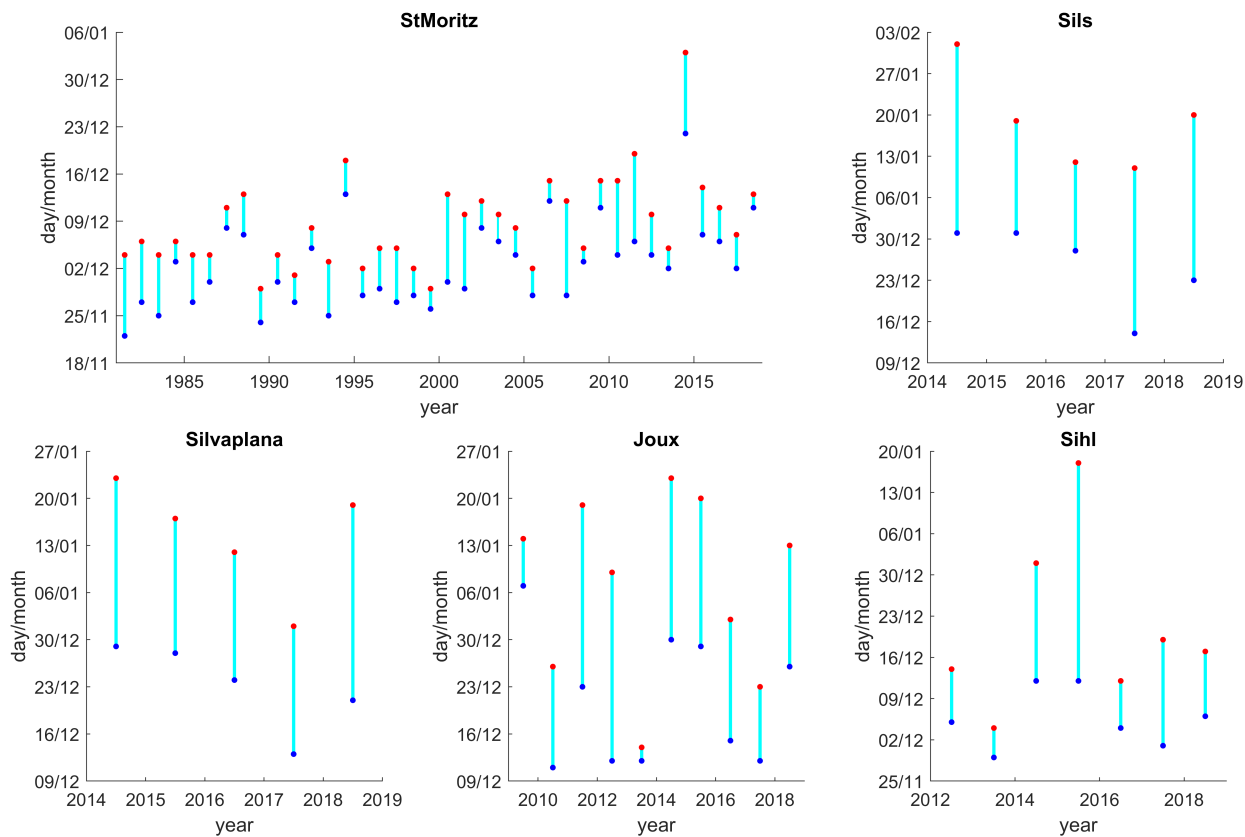


Figure S.5. Interannual variability of the pre-freezing period in Lakes St. Moritz, Sils, Silvaplana, Joux and Sihl, as simulated with Simstrat. Blue dots represent the day when homothermal conditions (water temperature reaching approximately 4°C along the whole water column) are reached; red dots the ice-on day.

S.5.2 Statistical distribution of the duration of the pre-freezing period

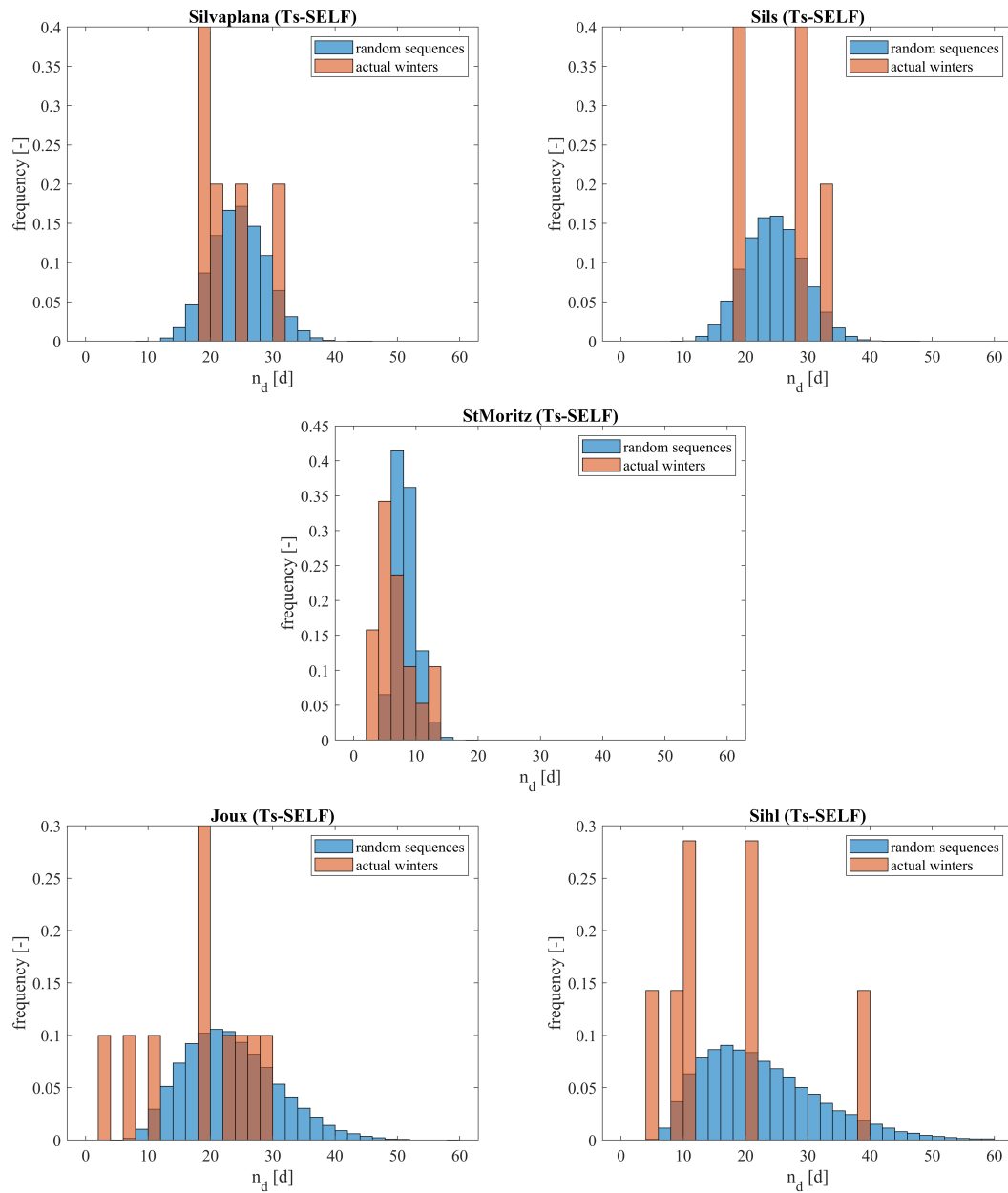


Figure S.6. Comparison among the statistical distribution of the duration of the pre-freezing period obtained by means of the 100'000 random runs with SELF and those simulated by Simstrat in the actual winters.

S.5.3 Results of the Monte Carlo analysis with SELF for the lakes not included in the main text

S.5.3.1 Lake Sils

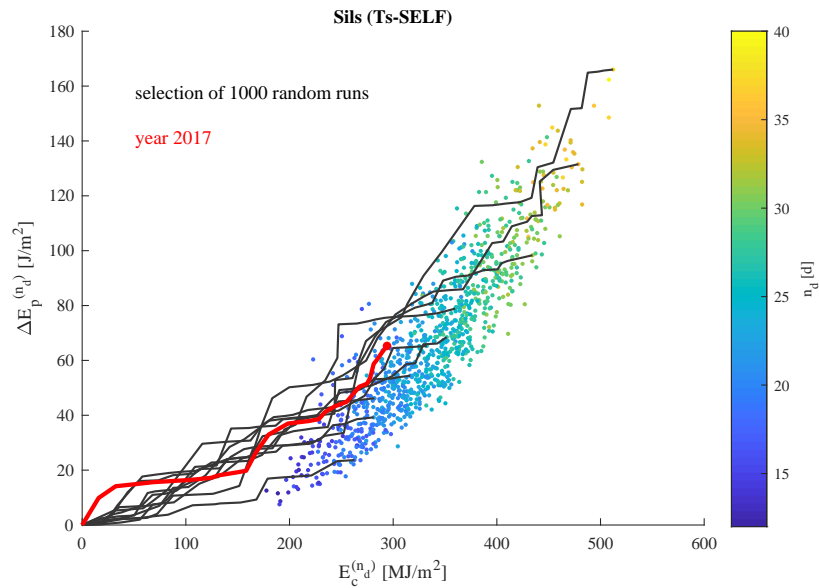


Figure S.7. Cumulative mixing energy $\Delta E_p^{(n_d)}$ vs. lost energy $E_c^{(n_d)}$ for Lake Sils. For notation, please refer to Figure 6 in the main text.

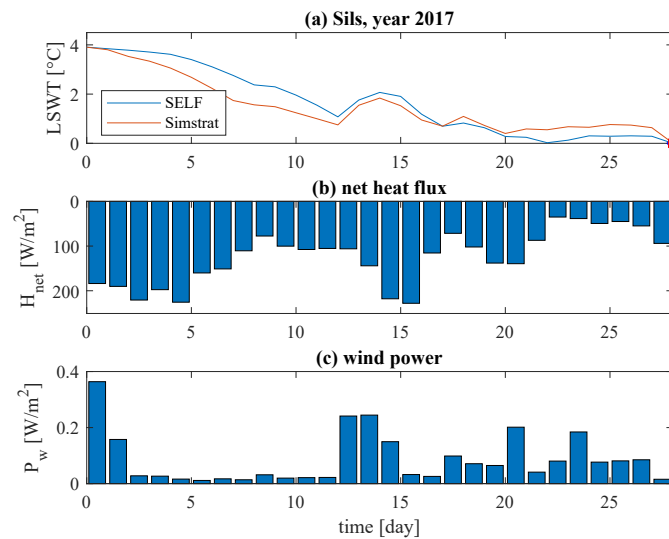


Figure S.8. Example of the dynamics in the pre-freezing period in Lake Sils. For notation, please refer to Figure 7 in the main text.

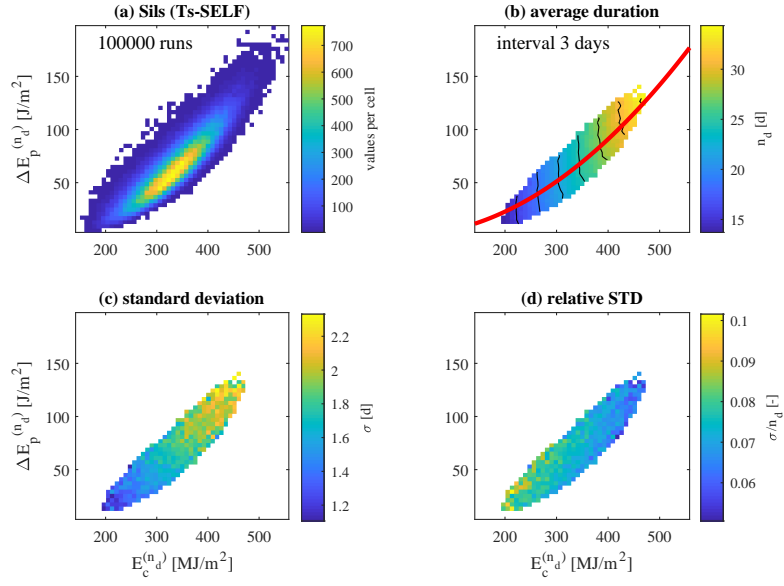


Figure S.9. Pre-freezing duration, in Lake Sils, depending on the cumulative values of the energies, $\Delta E_p^{(n_d)}$ and $E_c^{(n_d)}$. For notation, please refer to Figure 8 in the main text.

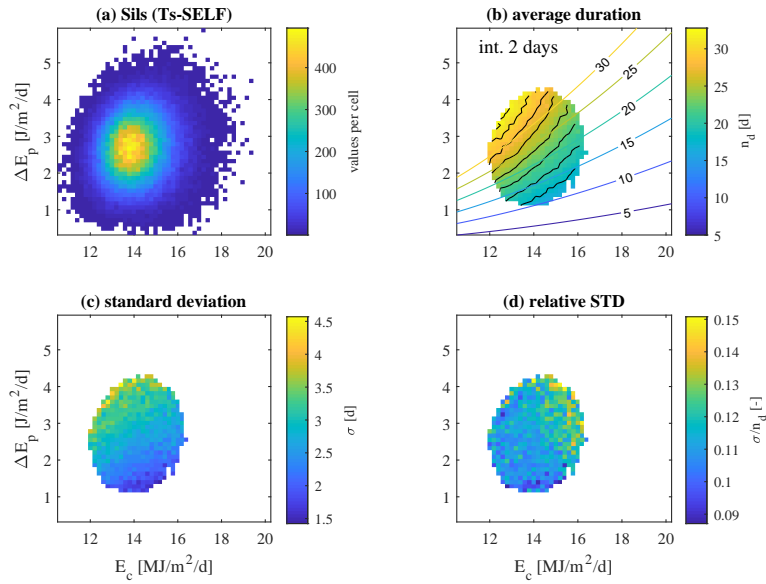


Figure S.10. Pre-freezing duration, in Lake Sils, depending on the average daily values of the energies, ΔE_p and E_c . For notation, please refer to Figure 9 in the main text.

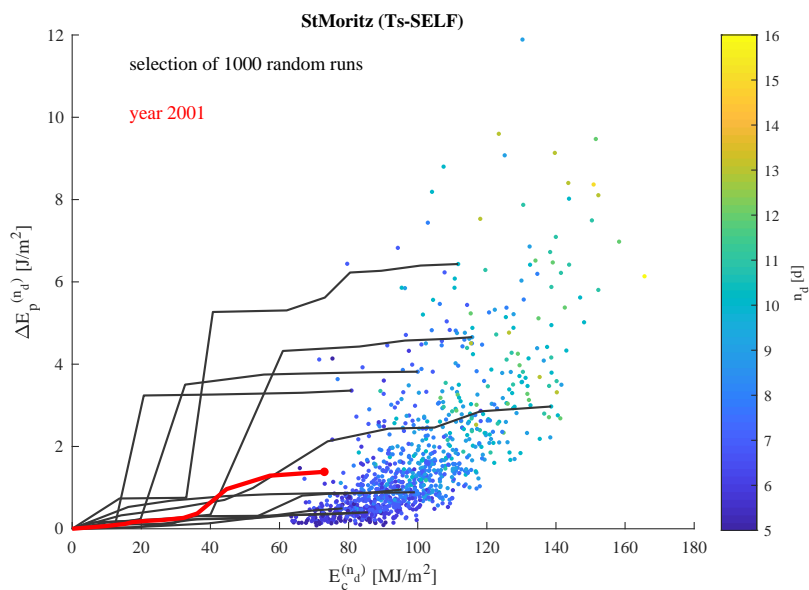


Figure S.11. Cumulative mixing energy $\Delta E_p^{(n_d)}$ vs. lost energy $E_c^{(n_d)}$ for Lake St. Moritz. For notation, please refer to Figure 6 in the main text.

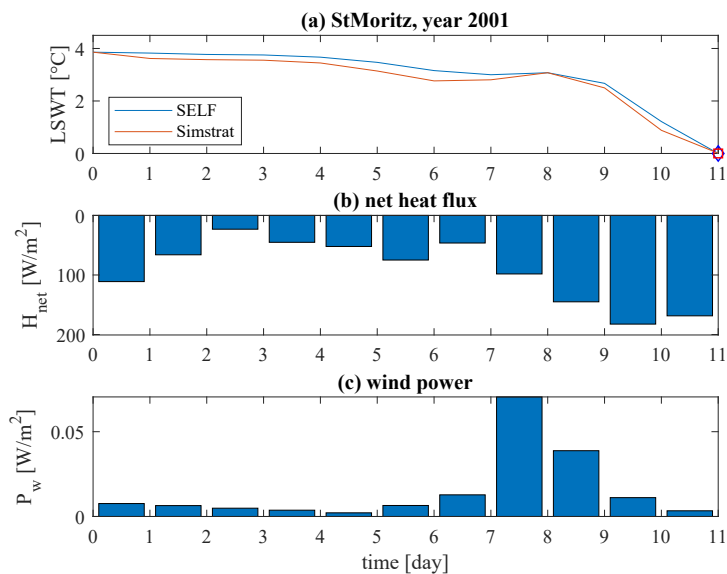


Figure S.12. Example of the dynamics in the pre-freezing period in Lake St. Moritz. For notation, please refer to Figure 7 in the main text.

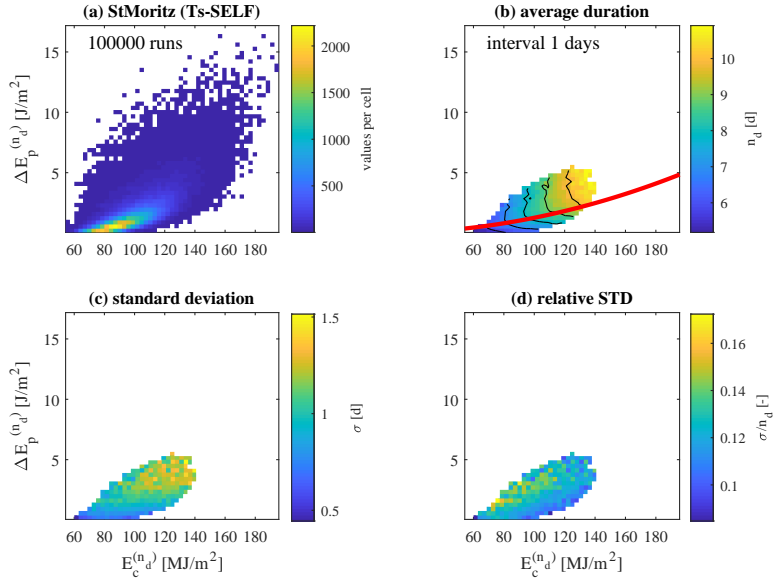


Figure S.13. Pre-freezing duration, in Lake St. Moritz, depending on the cumulative values of the energies, $\Delta E_p^{(n_d)}$ and $E_c^{(n_d)}$. For notation, please refer to Figure 8 in the main text.

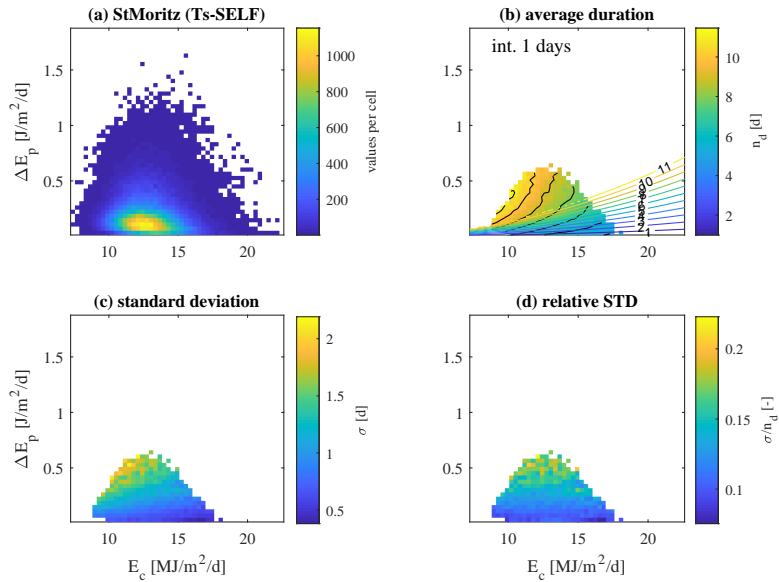


Figure S.14. Pre-freezing duration, in Lake St. Moritz, depending on the average daily values of the energies, ΔE_p and E_c . For notation, please refer to Figure 9 in the main text.

S.5.3.3 Lake Joux

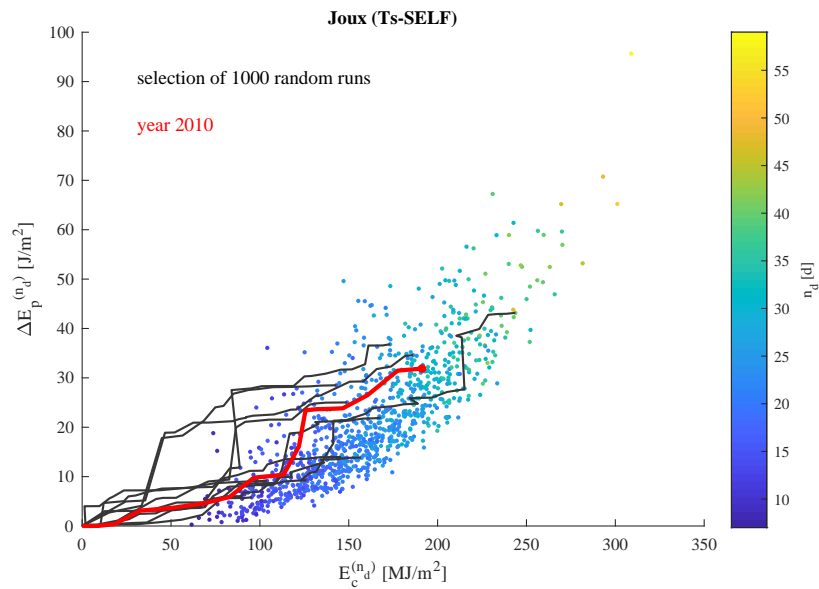


Figure S.15. Cumulative mixing energy $\Delta E_p^{(n_d)}$ vs. lost energy $E_c^{(n_d)}$ for Lake Joux. For notation, please refer to Figure 6 in the main text.

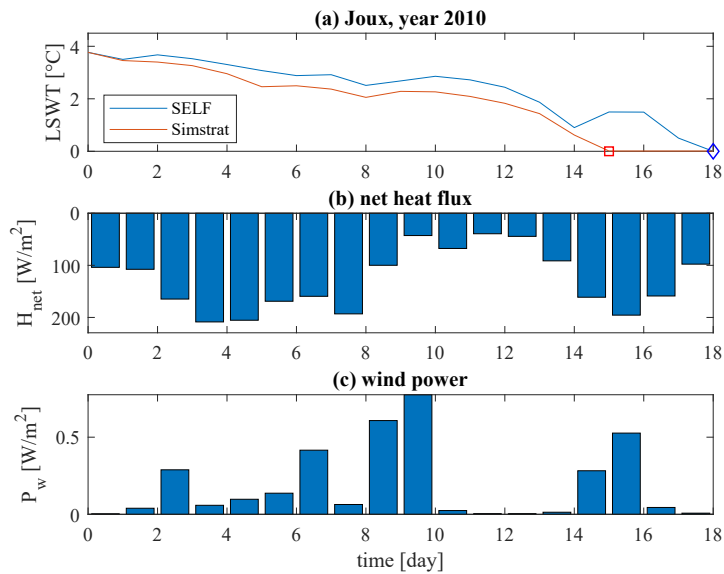


Figure S.16. Example of the dynamics in the pre-freezing period in Lake Joux. For notation, please refer to Figure 7 in the main text.

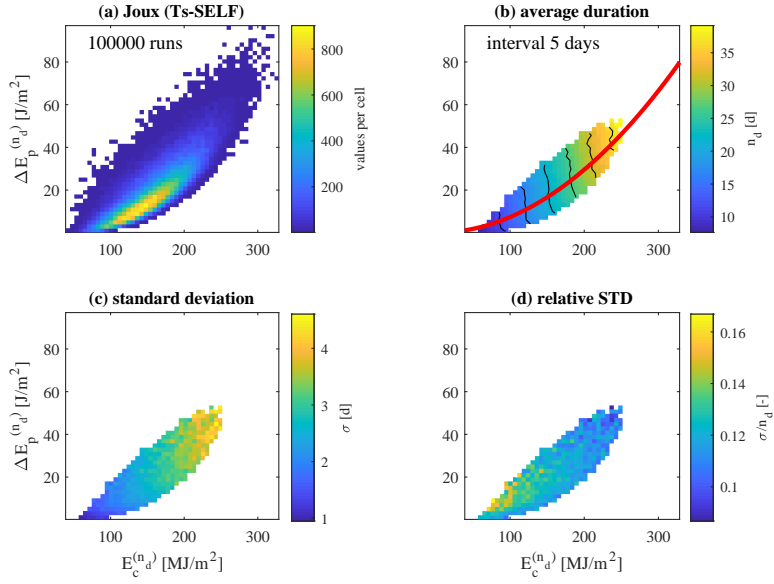


Figure S.17. Pre-freezing duration, in Lake Joux, depending on the cumulative values of the energies, $\Delta E_p^{(n_d)}$ and $E_c^{(n_d)}$. For notation, please refer to Figure 8 in the main text.

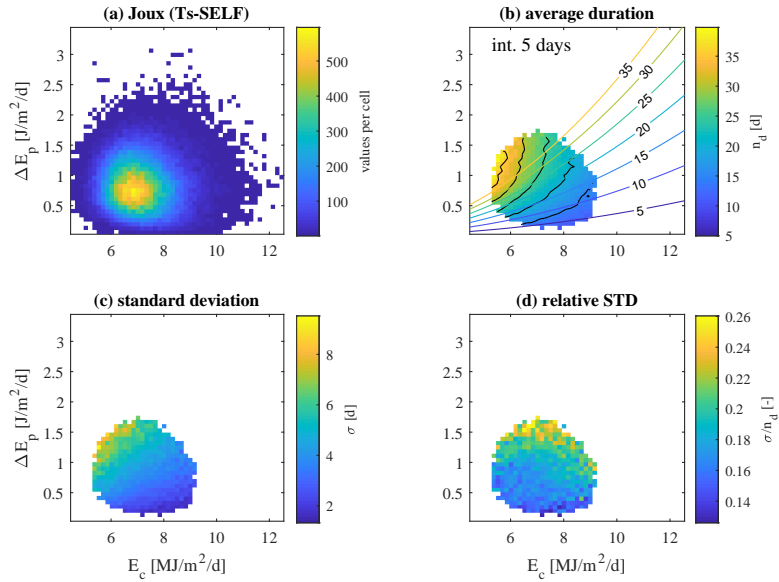


Figure S.18. Pre-freezing duration, in Lake Joux, depending on the average daily values of the energies, ΔE_p and E_c . For notation, please refer to Figure 9 in the main text.

S.5.3.4 Lake Sihl

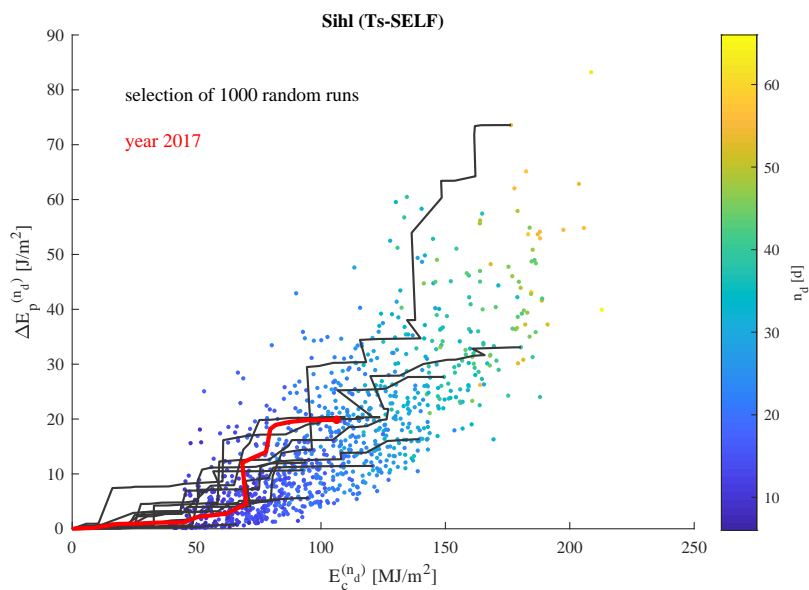


Figure S.19. Cumulative mixing energy $\Delta E_p^{(n_d)}$ vs. lost energy $E_c^{(n_d)}$ for Lake Sihl. For notation, please refer to Figure 6 in the main text.

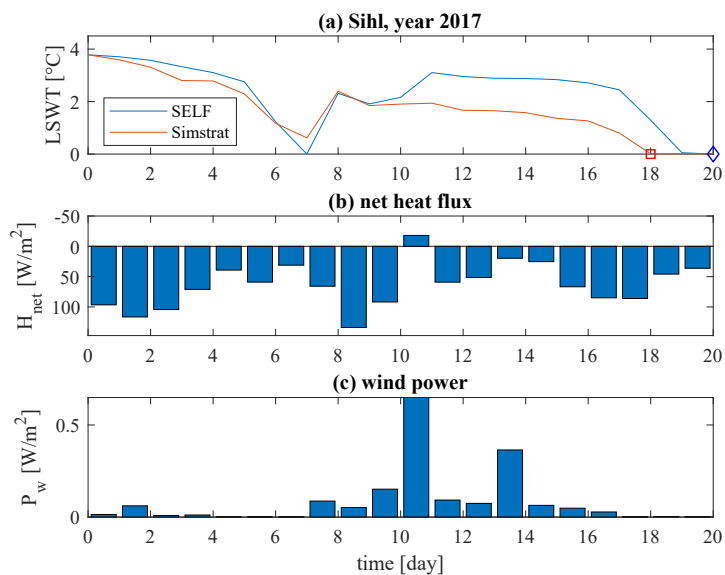


Figure S.20. Example of the dynamics in the pre-freezing period in Lake Sihl. For notation, please refer to Figure 7 in the main text.

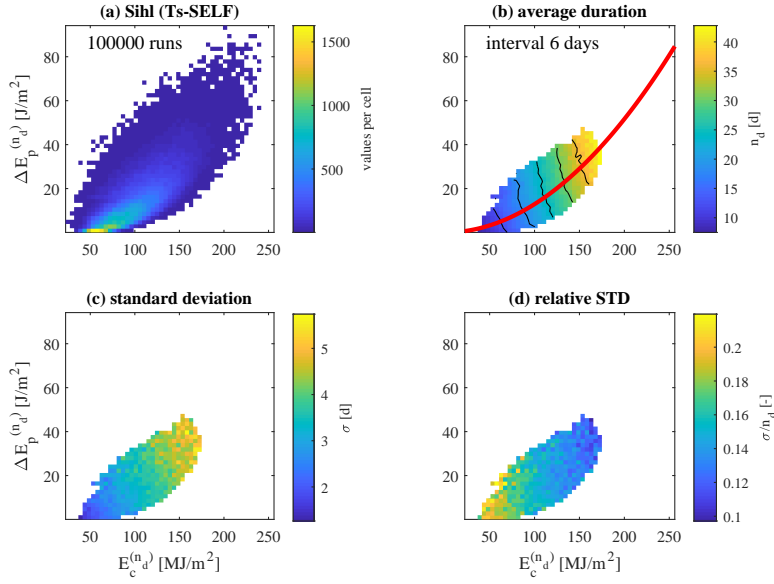


Figure S.21. Pre-freezing duration, in Lake Sihl, depending on the cumulative values of the energies, $\Delta E_p^{(n_d)}$ and $E_c^{(n_d)}$. For notation, please refer to Figure 8 in the main text.

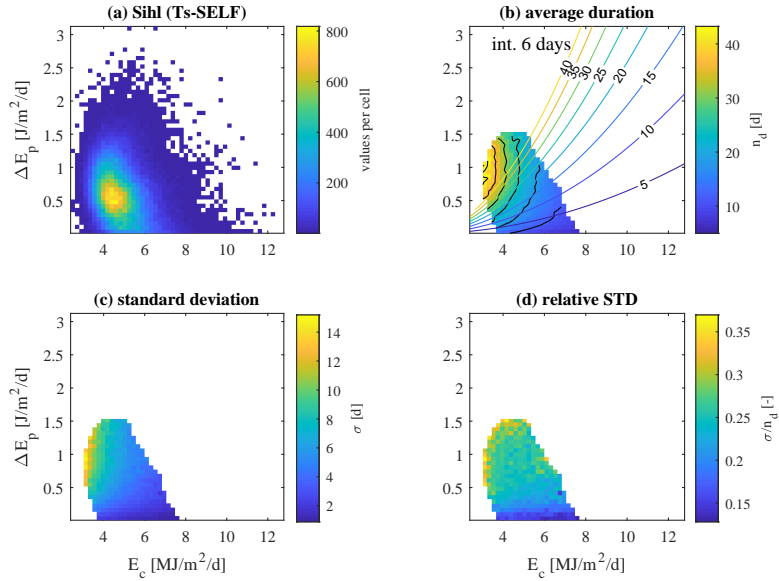


Figure S.22. Pre-freezing duration, in Lake Sihl, depending on the average daily values of the energies, ΔE_p and E_c . For notation, please refer to Figure 9 in the main text.

S.5.4 Correlation of the pre-freezing duration with negative degree days

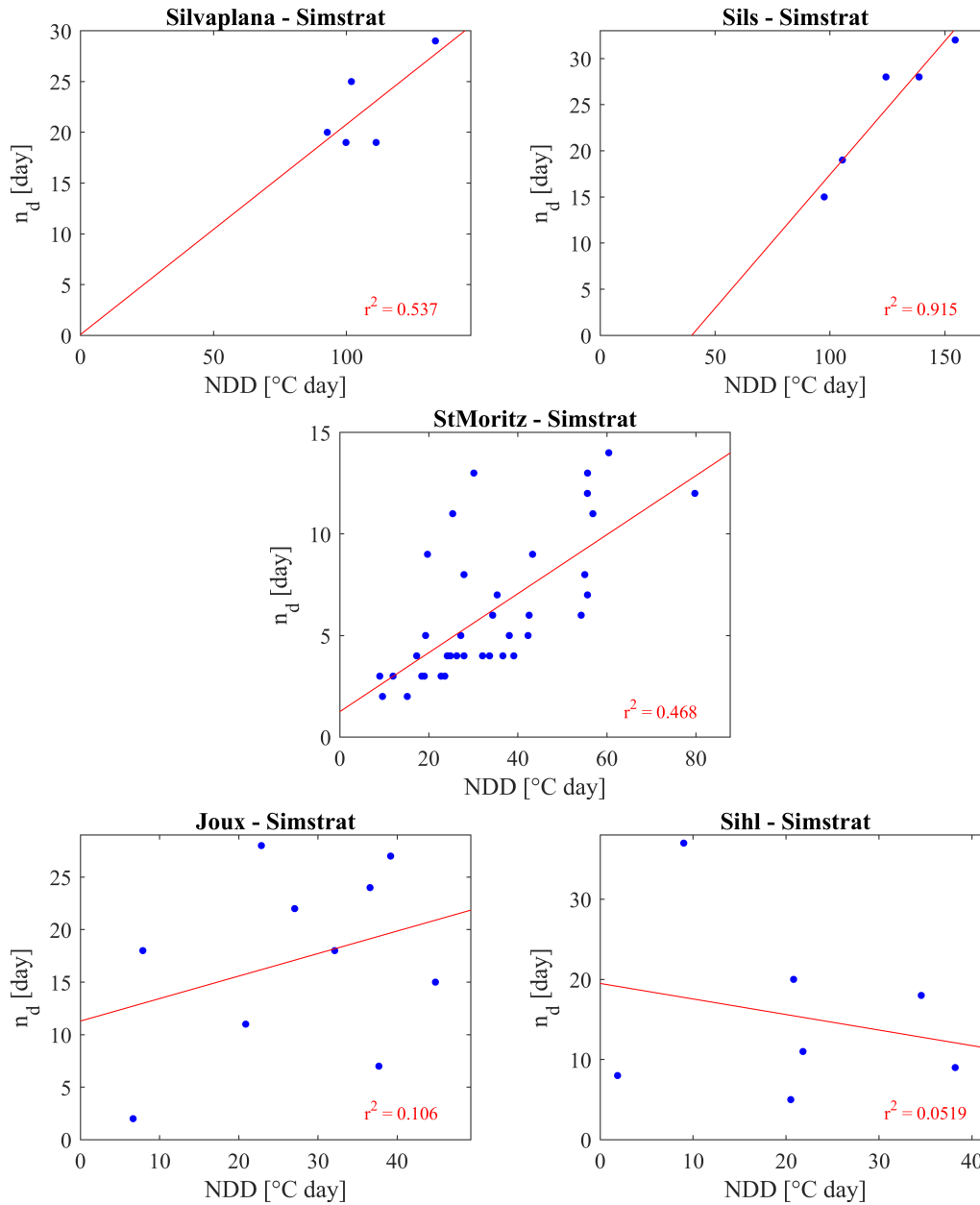


Figure S.23. Scatter plots of the duration of the pre-freezing period, n_d , vs the negative degree days (NDD). The red line represents the least-square linear fit, and the value of the Pearson correlation coefficient, r^2 , is shown in red within the plot. The quantities are obtained from the simulations run with Simstrat.

References

- 270 Goudsmit, G.-H., Burchard, H., Peeters, F., and Wüest, A.: Application of k - ϵ turbulence models to enclosed basins: The role of internal seiches, *J. Geophys. Res.*, 107, <https://doi.org/10.1029/2001JC000954>, 2002.
- Heaps, N.: Vertical structure of current in homogeneous and stratified waters, in: *Hydrodynamics of Lakes*, edited by Hutter, K., p. 153–207, Springer-Verlag, 1984.
- Imboden, D. and Wüest, A.: Mixing Mechanisms in Lakes, in: *Physics and Chemistry of Lakes*, edited by Lerman, A., Imboden, D., and
275 Gat, J., Springer-Verlag, 1995.
- Kullenberg, G. E. B.: On vertical mixing and the energy transfer from the wind to the water, *Tellus*, 28, 159–165, 1976.
- Simpson, J. H., Allen, C. M., and Morris, N. C. G.: Fronts on the continental shelf, *Journal of Geophysical Research: Oceans*, 83, 4607–4614, 1978.
- Toffolon, M. and Rizzi, G.: Effects of spatial wind inhomogeneity and turbulence anisotropy on circulation in an elongated basin: a simplified
280 analytical solution, *Advances in Water Resources*, 32, 1554–1566, <https://doi.org/10.1016/j.advwatres.2009.08.001>, 2009.
- Winters, K. B., Lombard, P. N., Riley, J. J., and D'Asaro, E. A.: Available potential energy and mixing in density-stratified fluids, *Journal of Fluid Mechanics*, 289, 115–128, <https://doi.org/10.1017/S002211209500125X>, 1995.
- Woolway, R. I. and Simpson, J. H.: Energy input and dissipation in a temperate lake during the spring transition, *Ocean Dynamics*, 67, 959–971, <https://doi.org/10.1007/s10236-017-1072-1>, 2017.